Cairo University

Journal of Advanced Research

ORIGINAL ARTICLE

# Dynamic light scattering of nano-gels of xanthan gum biopolymer in colloidal dispersion

CrossMark

Abbas Rahdar [a,b,]*, Mohammad Almasi-Kashi [a,c]

[a] *Institute of Nanoscience and Nanotechnology, University of Kashan, Kashan, P.O. Box 87317-51167, Islamic Republic of Iran*
[b] *Department of Physics, University of Zabol, Zabol, P.O. Box 35856-98613, Islamic Republic of Iran*
[c] *Department of Physics, University of Kashan, Kashan, P.O. Box 87317-51167, Islamic Republic of Iran*

G R A P H I C A L   A B S T R A C T
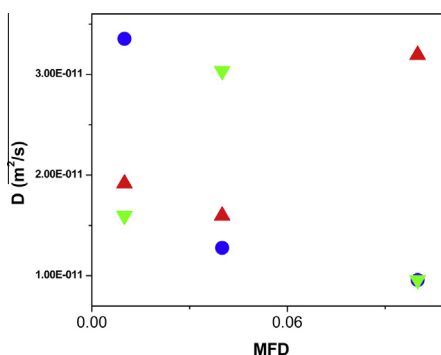
A R T I C L E   I N F O

A B S T R A C T

The dynamical properties of nanogels of xanthan gum (XG) with hydrodynamic radius controlled in a size range from 5 nm to 35 nm, were studied at the different XG concentrations in water/sodium bis-2-ethylhexyl-sulfosuccinate (AOT)/decane reverse micelles (RMs) vs. mass fraction of nano-droplet (MFD) at $W = 40$, using dynamic light scattering (DLS). The diffusion study of nanometer-sized droplets by DLS technique indicated that enhancing concentration of the XG polysaccharide resulted in exchanging the attractive interaction

* Corresponding author. Fax: +98 33482533.
E-mail addresses: a.rahdar@uoz.ac.ir, a.rahdarnanophysics@gmail.com (A. Rahdar).

between nano-gels to repulsive interaction, as the mass fraction of nano-droplets increased. The reorientation time (τ_r) of water nanodroplets decreased with MFD for water-in-oil AOT microemulsion comprising high concentration (0.0000625) of XG. On the other hand, decreasing concentration of biopolymer led to increasing the rotational correlation time of water nanodroplets with MFD. In conclusion, a single relaxation curve was observed for AOT inverse microemulsions containing different XG concentrations. Furthermore, the interaction between nanogels was changed from attractive to repulsive versus concentration of XG in the AOT RMs.

Introduction

Due to their tunable chemical properties, biocompatibility, and flexible three-dimensional physical structures, hydrogels or aquagels, networks of water-soluble polymers, are applied in various fields of study, including pharmaceutical engineering, biomaterials science, and biomedical engineering [1–4]. Nano-hydrocolloids in submicron dimensions are developed to obtain excellent advantages for drug delivery purposes via conjugating the polymeric networks with additives, such as drugs and proteins [5,6]. The synthesis of nano-sized hydrogels has attracted substantial attention in the recent years and different methods, such as biopolymers modification [7–11], free radical polymerization [12], microfluidics [13], and polymerization via reverse microemulsion [14–17] have been employed in the preparation of nanogels. The aforementioned methods have some deficiencies and superiorities. For instance, it was discovered through an eloquent series of studies that the exact controlling of the size of the hydrogels generated via the polymerization method in the inverse microemulsions avoids the variation in the hydrogel morphology and multi-steps synthesis present in other reported methods [7–13]. Moreover, different research groups have recently focused on the reverse micelles approach due to their wide application as a matrix to synthesize the nano-sized hydrogel particles and nano reactor for aqueous reactants [14–17].

These generated nanogels are networks of hydrophilic polymers, which are easily assembled in the aqueous core of reverse micelles. It is noteworthy that the size and shape of the nanogels obtained from the polymerization approach via the droplet reverse microemulsions are easily managed by the polar solvent-to-surfactant molar ratio [14–17]. In some practical applications, additives (i.e. drugs, DNA, magnetic particles, and cells) can be physically bonded inside the water nanodroplets, and these generated nanodroplets are stabilized via inclusion of a surface-active agent, such as AOT in bulk non-polar solvent to afford the final in reverse microemulsion [14–17]. Accordingly, the above-mentioned background, in the XG-loaded AOT reverse micelles (RMs), nano-sized water droplets containing XG (nanogels) are formed and dispersed by surfactant film of sodium di-2-ethylhexylsulfosuccinate (AOT, Aerosol OT) in the bulk apolar solvent of decane oil. Herein, the dynamic behavior of the AOT RM system contains polymer influenced by the interaction present between the polymer and the droplets or surfactant that in turn leads to adsorbing or non-adsorbing polymers in the water/surfactant interface or the water nano-droplet core, respectively [18–21]. Moreover, the length scale and molecular weight effects of different polymers on AOT RM system have been thoroughly

investigated [18–23]. However, the underlying details on preparation of nanogels of XG biopolymer at various concentrations in the water-in-decane AOT reverse micelle systems were not notified, to the best of the author's knowledge.

It is important to mention that XG is a hydrophilic polysaccharide with cellulose-like backbone fabricated by the *Xanthomonas campestris*. The preliminary structure of this biopolymer contains side chains and cellulose-like chain (Fig. 1) [24]. The anionic portion of XG biopolymer is due to the presence of the pyruvic and glucuronic groups in the side chains [25]. The XG is a biopolymer with a widespread range of usages in various fields, such as pharmaceutical, food, agricultural, and textile industries owing to its rheological properties. For instance, the XG has received a growing attention in various fields such as pharmaceutical formularization as a disintegrant, gelling agent, and binder because of its high viscosity at the polymer low concentrations. In addition, this polymeric species has been utilized as the key agent in the controlling and retarding process of drug release due to its gelling character and ability of encapsulating the drug within the gel as well as the drug delivery to the target area without creating a toxic effect [26]. Furthermore, the natural polysaccharides, such as xanthan and guar gums are selectively degraded in the colon, but not in the stomach and/or in small intestine [27]. Thus, utilizing these biopolymers in colon drug delivery is a good approach in treatment of colon-associated diseases [28]. Accordingly, in the present work, the dynamic of the nano-scale water droplets comprising XG in the water/AOT/decane RMs system at different XG concentrations and at $W = [\mathrm{H_2O/AOT}] = 40$ as a function of MFD using the DLS technique was investigated.

Experimental

Materials and preparation of entrapment–XG water nanodroplet (XG nanogels)

The AOT (purity > 99%), decane (purity > 95%), and XG were purchased from Sigma–Aldrich (Taufkirchen, Germany).

To prepare the AOT-templated nanogels of XG, the weighed powder of the biopolymer was initially dissolved in deionized water with a certain concentration (namely, 0.001) at room temperature. The polymer-to-water mass ratio, $Y = m_{\mathrm{polymer}}/m_{\mathrm{H2O}}$ [29], was specified as the concentration of XG in the AOT RMs. The water-containing AOT inverse micelles were prepared via mixing the appropriate mass value of the AOT, decane, and water containing different concentrations of XG at the fixed H$_2$O-to-AOT molar ratio ($W = 40$).
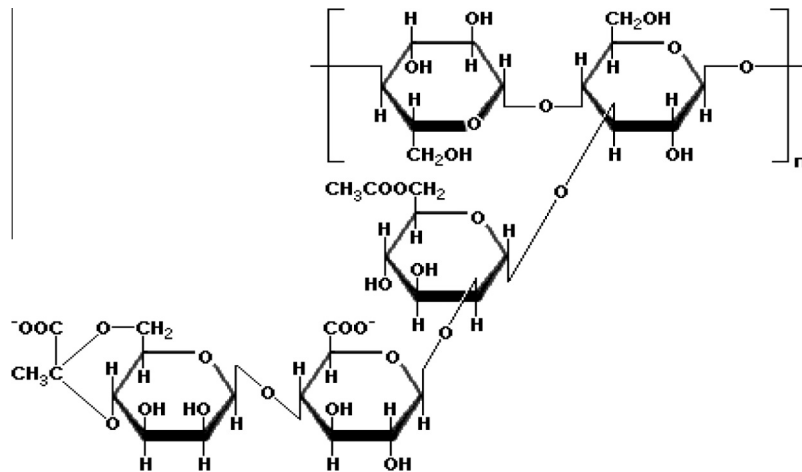
Fig. 1 Chemical structure of xanthan gum.

In the final step, the AOT RM was diluted with non-polar solvent of decane following the certain mass fraction of nano-droplet [29] at room temperature (RT).

Theory of dynamic light scattering

To study the inter-nanodroplet interactions by the collective diffusion coefficient of AOT nano-micelles, the DLS technique (also known as Quasi-Elastic Light Scattering (QELS)) or Photon Correlation Spectroscopy (PCS), was used to characterize the size distribution of nanometer-sized water droplets by a digital correlator [30–34]. The DLS technique utilized the time auto-correlation function to analyze the modulation of the scattered light intensity passing through a colloidal solution comprising submicron droplets. The scattered light intensity of AOT RMs was then monitored with time, which depends on the droplet size, Brownian motion of nano-droplets and their diffusive behavior in solution as well as viscosity of the continuous phase. Dynamic light scattering of the dispersed droplets was then investigated based on the fluctuation of the scattered intensity of $I(t)$. The autocorrelation function of the scattered light, $g^2(q, \tau)$, of AOT RMs was studied between the intensity of $I(t)$ at t and I [30–34] using the following Eq. (1).

$$g^2(\tau) = \frac{\langle I(t)I(t+\tau)\rangle}{\langle I(t)\rangle^2} \quad (1)$$

According to Eq. (1), the correlation between the signal intensities at t and $t + \tau$ increased as τ decreased and consequently $g^2(\tau)$ tends toward 1 [30–34]. The required time for decaying the auto-correlation function of micelles to zero was dependent on the size distribution of nano-droplets. Notably, the normalized auto-correlation function of $g^2(\tau)$ was related to the auto-correlation function of the scattered light electric field, $g^1(\tau)$, following the Siegert relationship [30–34].

$$g^2(\tau) - 1 = A|g^1(0)\exp(-DQ^2)|^2 \quad (2)$$

In which, A ($0 < A < 1$) was the experimental coherence factor, D was the diffusion coefficient and Q was the scattering vector. The magnitude of the scattering vector was related (Eq. (3)) to the wavelength of the X-ray or laser, the scattering angle of θ, and n, the refractive index of solvent [30–34].

$$Q = \frac{4\pi n}{\lambda}\sin\left(\frac{\theta}{2}\right) \quad (3)$$

Notably, when the particles were in mono-dispersed form, the autocorrelation function of $g^1(\tau)$, exhibited a single exponential decay curve [30–34].

$$g^1(\tau) = g^1(0)\exp(-DQ^2) \quad (4)$$

where DQ^2 defined as the inverse correlation time namely Γ [30–44].

$$D = \Gamma/Q2 \quad (5)$$

It is important to note that as the fluctuations in light intensity changed more slowly, increasing the sizes of droplets resulted in a slower relaxing exponential with a smaller relax constant, whereas decreasing the sizes of droplet led to a rapidly relaxing exponential function with a large relax constant. Therefore, the inverse correlation time is inversely proportional to the nano-droplet size [29–40].

Finally, the diffusion coefficient of AOT micelles was changed to the hydrodynamic radius following the Stokes-Einstein relation [30–34]:

$$r_h = \frac{K_B T}{6\eta\pi D} \quad (6)$$

in which, T was the temperature in K, K_B was a Boltzmann's constant, and η was the viscosity of the continuous phase in the AOT RMs.

The reorientation time, τ_r, for spherical droplets containing xanthan gum in the AOT reverse micelles was obtained based on the Stokes-Einstein-Debye (SED) relation [30–34].

$$\tau_r = \frac{4\pi\eta r_h^3}{3K_B T} \quad (7)$$

where K_B was Boltzmann's constant, r_h was the hydrodynamic radius of nano-scale droplets, T was the temperature in K, and η was the viscosity of the bulk phase in the water/AOT/decane microemulsion.

Results and discussion

The correlation function with relaxation time for W/O droplet microemulsions containing XG is depicted in Figs. 2–4. As

observed from Fig. 2, the auto-correlation function of micelle at MFD = 0.1, showed a shorter diffusion time compared with the other AOT reverse micelles. A through comparison of Figs. 2–4 revealed that the auto-correlation function of AOT water-in-oil microemulsion droplet at MFD = 0.1, exhibited shorter diffusion time compared with the other AOT reverse micelles. To obtain the relaxation rate, Γ, and the diffusion coefficient, D, of nano-scale water droplets, the auto-correlation function was fitted with a single exponential curve following Eq. (2). The relaxation rate of AOT inverse microemulsion versus MFD is shown in Fig. 1s. According to this figure, various concentrations of XG in the AOT water nanodroplets versus MFD resulted in changing the inverse correlation time of AOT RMs.

In general, it was found that by changing XG concentration in the AOT reverse micelles, variation of the size and diffusion of water droplets as well as the inter-nanogel interactions, versus mass fraction of droplet was observed. A careful analysis of diffusion of the AOT RMs comprising XG versus MFD, revealed that the collective diffusion for AOT micelles containing XG showed a negative slope as a function of MFD at concentration value of 0.0000079 and a positive slope at concentration of 0.0000625 (Fig. 5). Importantly, the nature of interaction of AOT droplets changed from attractive to repulsive force as concentration of XG biopolymer increased as a function of MFD. This observation was due to the fact that adsorbing XG polysaccharide at interfacial of AOT micelles, induced repulsive interaction of the droplet-droplet as a consequence of the increasing concentration of XG biopolymer in the AOT RMs [35,45]. On the other hand, non-adsorbing the XG biopolymer in core of droplets and decreasing the concentration of XG polysaccharide in the AOT RMs induced an attractive interaction between water droplets based on Asakura–Oosawa (AO) model of depletion interaction [35]. The fact that changing the size of droplet and the inter-droplet interactions affected changing content of oil in the RMs system has been proved by other research groups [29,36], thus further supporting the current observations.

It is worth to note that in the spherical water-comprising AOT reverse micelles, H_2O/AOT interactions were less desirable than H_2O/H_2O and/or AOT/AOT interactions due to size
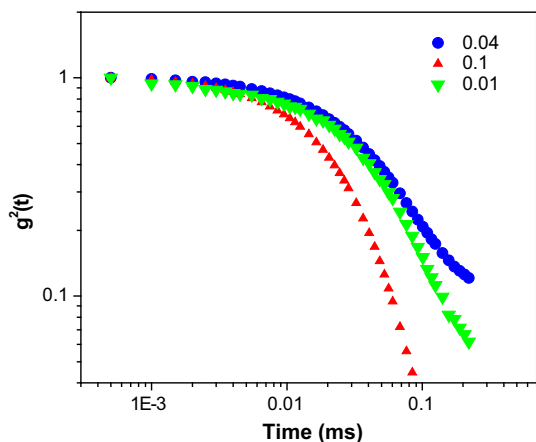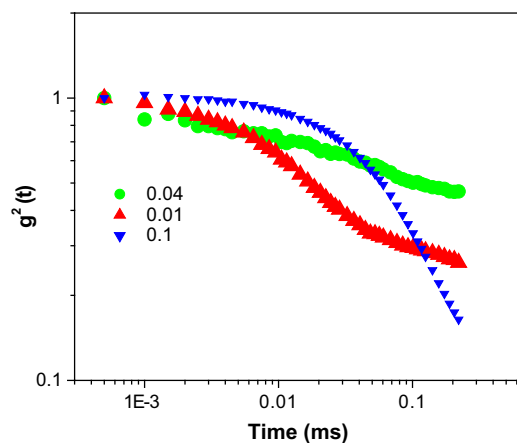

Fig. 3 The autocorrelation function versus time for AOT reversed nano-micelles at polymer concentration of 0.0000157 at RT.
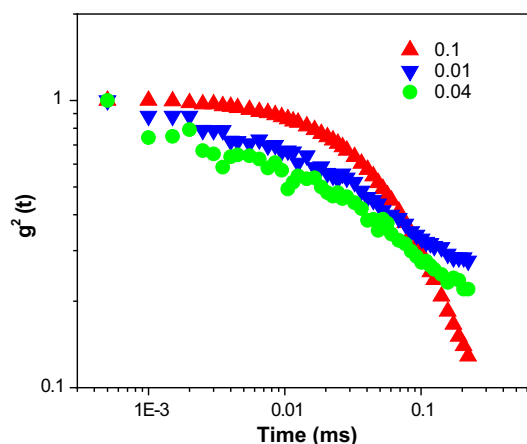

Fig. 4 The autocorrelation function versus time for AOT reverse nano-micelles at polymer concentration of 0.0000079 at RT.
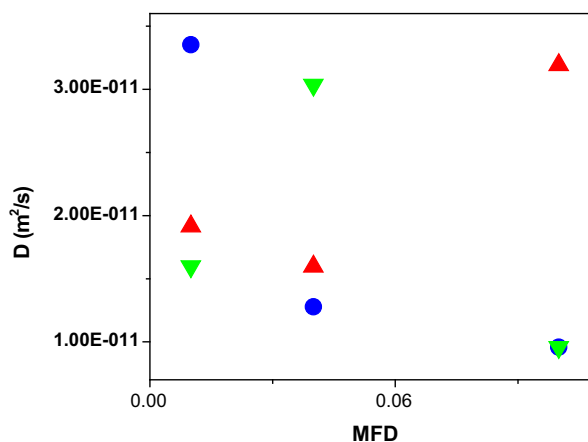

Fig. 5 Diffusion coefficient of AOT RMs containing different xanthan gum concentrations as a function of MFD (up triangle): 0.0000625, (circle): 0.0000157 and (down triangle): 0.0000079 at RT.

Fig. 2 The autocorrelation function versus time for AOT reversed nano-micelles at polymer concentration of 0.0000625 at RT.

effects in the nanometer-sized structures [42,43]. It is well known that both sizes and interactions of water-soluble macromolecules affected the dynamics of water droplets in Reverse micelles [44,45]. As observed in Fig. 6, the average size of nanogels was determined by interpreting the diffusion coefficient of micelles, as the hydrodynamic radius using the Stokes-Einstein relation. As is apparent in Fig. 6, the hydrodynamic size of water droplets decreased as polysaccharide concentration of XG increased in the AOT inverse microemulsion. Notably, change of size of the micellar core via adding an additive in the water-comprising AOT reversed micelles has been reported by others [29,41].

To support this phenomena, it was proposed that (i) biopolymer of XG acted as co-surfactants; thus, by increasing the concentration of the XG biopolymer in the AOT RMs, the interfacial surface of AOT micelles increased. This led to enhancing the number of water nanodroplets and decreasing their sizes, as observed experimentally. (ii) Some parts of XG or their ends may be adsorbed to the surface of the AOT molecules as an active agent at the interfacial of AOT micelles, while the other parts may be non-adsorbed in the core of water droplets. After this observation, the elastic energy of XG molecules may result in decreasing the size of the droplets [37,38]. (iii) Furthermore, reduction in droplet sizes was attributed to decrease in overlapping the interface domain of inter-droplets, which in turn causes the decreased strength of the attractive interaction [37,38]. If the elastic modulus as only factor in change of the droplets size to be considered, therefore, the nano-droplet sizes decreased as the interface curvature increased due to the surface-to-volume effects in nano-scale systems [39].

The size distribution of AOT nanometer-sized water droplet comprising the different xanthan gum concentration obtained from DLS measurement with MFD is shown in Figs. 2–4s.

The reorientation time (τ_r) of water nano-droplets containing the xanthan gum biopolymer versus MFD achieved by the Stokes-Einstein-Debye (SED) relation is also shown in Fig. 7. As observed, changing the reorientation time of micelles upon an external perturbation such as inclusion of an additive
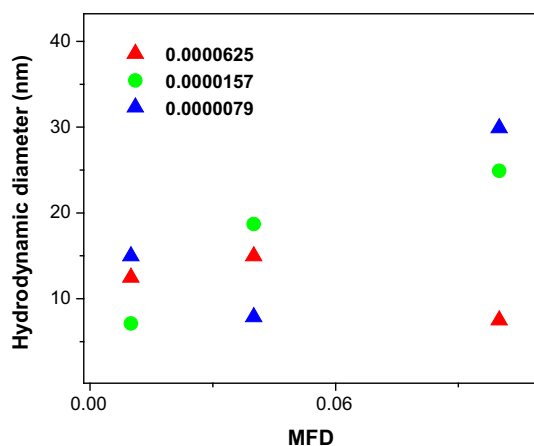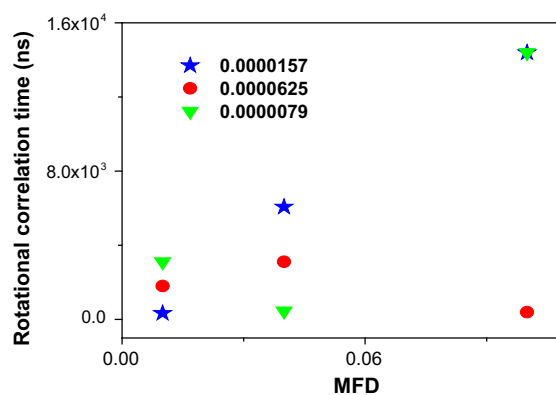

Fig. 7 Rotational correlation time (τ_r) versus MFD for water nano-droplets containing different concentrations of XG in AOT RM at concentration (circle): 0.0000625, (star):0.0000157 and (down triangle):0.0000079 using the SED relation.

resulted in changing in fluidity of a system well [40]. Moreover, according to this figure, for AOT water-in-oil droplet microemulsion containing XG with high concentration (0.0000625), the reorientation time (τ_r) of water nanodroplets decreased with MFD, whereas decreasing the concentration of biopolymer, the rotational correlation time of water nanodroplets increased versus mass fraction of water nanodroplet.

Conclusions

To sum up, the diffusion of nano-scale hydrogels comprising the different XG concentrations at the H_2O-to-AOT molar ratio of 40 ($W = 40$) and different mass fraction of nano-droplets was studied by dynamic light scattering technique in water-in-decane droplet microemulsion. The nano-gels were formed and dispersed in the bulk phase of decane based on the anionic surfactant of AOT (sodium bis[2-ethylhexyl] sulfosuccinate). A single relaxation curve was observed for nanogels, further supporting the fact that addition of XG to the water-comprising AOT reversed micelles. As highlighted by the analysis of dynamic light scattering of micelles, with increasing the concentration of the XG biopolymer, the diffusion coefficient of nanogels increased and size of droplets decreased as mass fraction of droplets increased. Lastly, it was found that enhancing the concentration of XG in the AOT micelles changed the nature of inter-nanogels interaction from an attractive to repulsive force.

Conflict of Interest

The authors have declared no conflict of interest.

Compliance with Ethics Requirements

This article does not contain any studies with human or animal subjects.

Fig. 6 Hydrodynamic diameter of AOT water nanodroplets containing different xanthan gum concentrations using Stokes-Einstein Relation versus MFD (up triangle): 0.0000625, (circle): 0.0000157 and (down triangle): 0.0000079, at RT.

Appendix A. Supplementary material

Supplementary data associated with this article can be found, in the online version, at http://dx.doi.org/10.1016/j.jare.2016.06.009.

References

[1] Ahmed EM. Hydrogel: preparation, characterization, and applications: a review. J Adv Res 2015;6(2):105–21.

[2] Deligkaris K, Tadele TS, Olthuis W, van den Berg A. Hydrogel-based devices for biomedical applications. Sensor Actuat B – Chem 2010;147(2):765–74.

[3] Hoffman AS. Hydrogels for biomedical applications. Adv Drug Deliv Rev 2002;54(1):3–12.

[4] Hoare TR, Kohane DS. Hydrogels in drug delivery: progress and challenges. Polymer 2008;49(8):1993–2007.

[5] Harris JM, Chess RB. Effect of pegylation on pharmaceuticals. Nat Rev Drug Discov 2003;2(3):214–21.

[6] Vicent MJ, Greco F, Nicholson RI, Paul A, Griffiths PC, Duncan R. Polymer therapeutics designed for a combination therapy of hormone-dependent cancer. Angew Chem Int Ed Engl 2005;44(26):4061–6.

[7] Nishikawa T, Akiyoshi K, Sunamoto J. Macromolecular complexation between bovine serum albumin and the self-assembled hydrogel nanoparticle of hydrophobized polysaccharides. J Am Chem Soc 1996;118(26):6110–5.

[8] Nishikawa T, Akiyoshi K, Sunamoto J. Supramolecular assembly between nanoparticles of hydrophobized polysaccharide and soluble protein complexation between the self-aggregate of cholesterol-bearing pullulan and alpha-chymotrypsin. Macromolecules 1994;27(26):7654–9.

[9] Lee I, Akiyoshi K. Single molecular mechanics of a cholesterol-bearing pullulan nanogel at the hydrophobic interfaces. Biomaterials 2004;25(15):2911–8.

[10] Akiyoshi K, Kang EC, Kurumada S, Sunamoto J, Principi T, Winnik FM. Controlled Association of amphiphilic polymers in water: thermosensitive nanoparticles formed by self-assembly of hydrophobically modified pullulans and Poly(N-isopropylacrylamides). Macromolecules 2000;33(9):3244–9.

[11] Bodnar M, Hartmann JF, Borbely J. Synthesis and study of cross-linked chitosan-N-poly(ethylene glycol) nanoparticles. Biomacromolecules 2006;7(11):3030–6.

[12] Ma Z, Lacroix-Desmazes P. Dispersion polymerization of 2-hydroxyethyl methacrylate stabilized by a hydrophilic/CO 2-philic poly(ethylene oxide)-b-poly(1, 1, 2, 2-tetrahydroperfluorodecyl acrylate)(PEO-b-PFDA) diblock copolymer in supercritical carbon dioxide. Polymer 2004;45(20):6789–97.

[13] Zhang H, Tumarkin E, Sullan RMA, Walker GC, Kumacheva E. Exploring microfluidic routes to microgels of biological polymers. Macromol Rapid Commun 2007;28(5):527–38.

[14] Oh JK, Siegwart DJ, Lee HI, Sherwood G, Peteanu L, Hollinger JO, et al. Biodegradable nanogels prepared by atom transfer radical polymerization as potential drug delivery carriers: synthesis, biodegradation, in vitro release, and bioconjugation. J Am Chem Soc 2007;129(18):5939–45.

[15] Mitra S, Gaur U, Ghosh PC, Maitra AN. Tumour targeted delivery of encapsulated dextran-doxorubicin conjugate using chitosan nanoparticles as carrier. J Control Release 2001;74(1–3):317–23.

[16] Lee H, Mok H, Lee S, Oh YK, Park TG. Target-specific intracellular delivery of siRNA using degradable hyaluronic acid nanogels. J Control Release 2007;119(2):245–52.

[17] McAllister K, Sazani P, Adam M, Cho MJ, Rubinstein M, Samulski RJ, et al. Polymeric nanogels produced via inverse microemulsion polymerization as potential gene and antisense delivery agents. J Am Chem Soc 2002;124(51):15198–207.

[18] Meier W. Poly(oxyethylene) adsorption in water/oil microemulsions: a conductivity study. Langmuir 1996;12(5):1188–92.

[19] Laia CA, Brown W, Almgren M, Costa SM. Light scattering study of water-in-oil AOT microemulsions with poly(oxy) ethylene. Langmuir 2000;16(2):465–70.

[20] Maugey M, Bellocq AM. Effect of added salt and poly(ethylene glycol) on the phase behavior of a balanced AOT−water−oil system. Langmuir 1999;15(25):8602–8.

[21] Papoutsi D, Lianos P, Brown W. Interaction of polyethylene glycol with water-in-oil microemulsions. 3. Effect of polymer size and polymer concentration. Langmuir 1994;10(10):3402–5.

[22] Milas M, Rinaudo M. Properties of xanthan gum in aqueous solutions: role of the conformational transition. Carbohyd Res 1986;158:191–204.

[23] Li H, Chen R, Lu X, Hou W. Rheological properties of aqueous solution containing xanthan gum and cationic cellulose JR400. Carbohyd Polym 2012;90(3):1330–6.

[24] Katzbauer B. Properties and applications of xanthan gum polymer degradation and stability. Polym Degrad Stab 1998;59(1):81–4.

[25] Kwon GS, Moon SH, Hong SD, Lee HM, Mheen TI, Oh HM, et al. Rheological properties of extracellular polysaccharide, Pestan, produced by Pestalotiopsis sp. Biotechnol Lett 1996;18(12):1465–70.

[26] Benny IS, Gunasekar V, Ponnusami V. Review on application of xanthan gum in drug delivery. Int J PharmTech Res 2014;6(4):1322–6.

[27] Salyers AA, Vercellotti JR, West SE, Wilkins TD. Fermentation of mucin and plant polysaccharides by strains of bacteroides from the human colon. Appl Environ Microbiol 1977;32(2):319–22.

[28] Ramasamy T, Kandhasami UD, Ruttala H, Shanmugam S. Formulation and evaluation of xanthan gum based aceclofenac tablets for colon targeted drug delivery. Braz J Pharm Sci 2011;47(2):299–311.

[29] Rahdar A, Almasi-Kashi M. Photophysics of Rhodamine B in the nanosized water droplets: a concentration dependence study. J Mol Liq 2016;220:395–403.

[30] Brown W. Dynamic light scattering: the method and some applications. Oxford: Clarendon Press; 1993.

[31] Finsy R. Particle sizing by quasi-elastic light scattering. Adv Colloid Interface Sci 1994;52:79–143.

[32] Pecora P. Dynamic light scattering applications of photon correlation spectroscopy. New York: Plenum Press; 1985.

[33] Zhu R, Lu R, Yu A. Photophysics and locations of IR125 and C152 in AOT reverse micelles. Phys Chem Chem Phys 2011;13(64):20844–54.

[34] Valeur B, Berberan-Santos MN. Molecular fluorescence: principles and applications. 2nd ed. Germany: Wiley-VCH; 2012.

[35] Cosgrove T. Colloid Science: principles, methods and applications. 2nd ed. United Kingdom: John Wiley and Sons; 2010.

[36] Florez Tabares JS, Correa NM, Silber JJ, Sereno LE, Molina PG. Droplet–droplet interactions investigated using a combination of electrochemical and dynamic light scattering techniques. The case of water/BHDC/benzene: n-heptane system. Soft Matter 2015;11(15):2952–62.

[37] Suarez MJ, Lang J. Effect of Addition of water-soluble polymers in water-in-oil microemulsions made with anionic and cationic surfactants. J Phys Chem 1995;99(13):4626–31.

[38] Suarez MJ, Levy H, Lang J. Effect of addition of polymer to water-in-oil microemulsions on droplet size and exchange of material between droplets. J Phys Chem 1993;97(38):9808–16.

[39] Stubenrauch C. Microemulsions: background, new concepts, applications, perspectives. 1st ed. United Kingdom: John Wiley and Sons; 2009.

[40] Eastoe J, Young WK, Robinson BH, Steytler DC. Scattering studies of microemulsions in low-density alkanes density alkanes. J Chem Soc Faraday Trans 1990;86(16):2883–9.

[41] Israelachvili JN, Mitchell DJ, Ninham BW. Theory of self-assembly of hydrocarbon amphiphiles into micelles and bilayers. J Chem Soc Faraday Trans 2 – Mol Chem Phys 1976;72:1525–68.

[42] Oakenfull D. Constraints of molecular packing on the size and stability of microemulsion droplets. J Chem Soc Faraday Trans 1 1980;76:1875–86.

[43] Luisi PL, Magid LJ, Fendler JH. Solubilization of enzymes and nucleic acids in hydrocarbon micellar solution. Crit Rev Biochem 1986;20(4):409–74.

[44] Luisi PL. Enzyme als Gastmoleküle in inversen Micellen. (1985). Angew Chem 1985;97:449–60.

[45] Bellocq AM. Phase equilibria of polymer-containing microemulsions. Langmuir 1998;14(14):3730–9.